Simulation-Based Calibration Verification for (Sub-)Terahertz *S*-Parameter Measurements

Sang-Hee Shin, *Member, IEEE*, Stepan Lucyszyn, *Fellow, IEEE*, and Nick M. Ridler, *Fellow, IEEE*

***Abstract*—This article presents a cost-effective method for verifying (sub-)terahertz scattering (*S*-)parameter measurements using a vector network analyzer (VNA) with frequency extension modules. The approach reduces the need for physical standards with rigorous dimensional characterization by using full-wave electromagnetic (EM) simulation to create a "simulation-driven reference model" with a predictable uncertainty envelope. This method utilizes the known manufacturing tolerances of generic waveguide sections to generate a pass/fail verification bound. Two simple, calculable waveguide devices (a cross-connected line and reduced-aperture sections) are characterized in the WM-570 (330–500 GHz) band. Excellent agreement is achieved between the EM-simulated predictions and VNA-measured *S*-parameters, with the measurements falling within the calculated uncertainty bounds. This work demonstrates that combining simple hardware with EM simulation is a reliable and low-cost approach for validating *S*-parameter measurements and calibrations at terahertz frequencies.**

***Index Terms*—*S*-parameters, terahertz (THz), vector network analyzer (VNA), waveguide, WM-570.**

I. Introduction

There is an accelerating increase of interest in millimeter-wave and terahertz technologies, for applications requiring large bandwidths such as 5G/6G+ telecommunications, security stand-off detection, and defense. To this end, the importance of accurate measurement at these frequencies is becoming more significant. At (sub-)THz frequencies, metal-pipe rectangular waveguides (MPRWGs) are a primary medium for low-loss signal transmission. Their performance is typically characterized by using a vector network analyzer (VNA), equipped with frequency extension modules. Producing reliable results with this instrumentation requires accurate calibration and subsequent verification to confirm the measurement system's accuracy [1].

A crucial step in this process is the use of verification standards for independent post-calibration validation. Typically, the verification standards can be devices with S-parameters that are accurately predictable from their physical dimensions. While devices such as cross-connected waveguides (CCWs) [2] and reduced aperture waveguides (RAWs) [3] have been shown to be effective for this purpose at lower millimeter (mm-)wave frequencies, this approach encounters significant challenges at (sub-)THz frequencies. As device dimensions reduce to the sub-millimeter scale, precision manufacturing becomes considerably more difficult and costly. At these short wavelengths, even minor fabrication errors, such as dimensional deviations in the waveguide's aperture or misalignment between flanges, can become a significant fraction of the operating wavelength and begin to dominate the overall measurement uncertainty. Moreover, dimensional analysis for characterizing verification standards requires higher levels of precision and accuracy.

To overcome these challenges, this article demonstrates a simulation-driven verification strategy. Conventionally, verification standards require rigorous physical characterization, such as dimensional metrology performed by a National Metrology Institute (NMI), to establish their "true" S-parameters. While highly accurate, this process is expensive and often impractical for most end-users.

This work proposes a cost-effective alternative: a "simulation-driven reference model." Instead of characterizing the specific physical dimensions of a manufactured artifact, we utilize full-wave electromagnetic (EM) simulations, based on the nominal manufacturing tolerances of a waveguide class. This generates a probabilistic uncertainty envelope. If the measured S-parameters of a commercial device fall within this calculated envelope, the measurement system can be considered verified within those bounds. This approach serves as a cost-effective and reliable verification technique for routine laboratory measurements where rigorous primary-level accuracy is not required.

In this work, two specific examples are considered: a cross-connected device, realized by rotating a WM-570 line standard by 90°, and reduced-aperture devices, formed by inserting a section of WM-380 waveguide between the WM-570 reference planes. This simulation-driven approach provides a convenient solution to the inherent challenges of (sub-)THz measurement verification.

II. Calibration and Verification

A. Calibration

For two-port S-parameter measurements, techniques such as thru-reflect-match (TRM) [4], thru-reflect-line (TRL) [5],

Received 8 December 2025; accepted 18 January 2026. Date of publication 6 February 2026; date of current version 20 February 2026. This work was supported in part by the U.K. Government's Department for Science, Innovation and Technology (DSIT); and in part by the Institute of Information and Communications Technology Planning and Evaluation (IITP)-Information Technology Research Center (ITRC) IITP grant funded by Korean Government (Ministry of Science and Information and Communication Technology) under Grant IITP-2024-RS-2024-00437191. The Associate Editor coordinating the review process was Dr. Michael Gadringer. *(Corresponding author: Sang-Hee Shin.)*

Sang-Hee Shin is with Sungkyunkwan University, Suwon 16419, South Korea (e-mail: ssh1625@skku.edu).

Stepan Lucyszyn is with Imperial College London, SW7 2AZ London, U.K. (e-mail: s.lucyszyn@imperial.ac.uk).

Nick M. Ridler is with the National Physical Laboratory, TW11 0LW Teddington, U.K. (e-mail: nick.ridler@npl.co.uk).

Digital Object Identifier 10.1109/TIM.2026.3661688

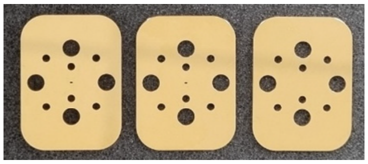

Fig. 1. WM-570 calibration standards. Long line (left), short line (center), and flush short (right).

and line-reflect-line (LRL) [4] are commonly employed for calibrating VNAs. At (sub-)millimeter wave frequencies, TRM and LRL are common but necessitate the accurate pre-characterization of at least one standard. Here, the TRL calibration scheme was employed, as it requires no pre-defined standards—only that the reflect standards for both ports are identical [1].

A challenge arises with traditional TRL at these high frequencies. The method typically employs a quarter-wavelength (1/4-wave) line standard, which provides an in-band phase change between 20° and 160° [6]. However, for the WM-570 band, the line standard would be physically too thin (less than 200 μm), compromising its mechanical integrity. As a more robust alternative, this work employs 3/4-wave lines, which are physically thicker and provide a suitable phase delay between 210° and 330° [7]. Here, two line standards were used, manufactured by Swiss-to-12, to cover the full frequency range: a 951 μm line for 330–394 GHz; and a 651 μm line for 380–500 GHz. A flush short from the same manufacturer was used as the reflect standard. To achieve a seamless full-band calibration, the S-parameter results from these two frequency ranges were merged using a weighting scheme [8]. The calibration standards employed in this study are shown in Fig. 1.

B. Verification Standard and Uncertainty Prediction

The geometry and features of the verification device must be simple enough to be accurately calculable using mathematical or computational analysis.

In this study, a CCW and RAWs were chosen, as they are passive components with very simple geometry. Full-wave EM simulation using CST Microwave Studio is used to predict the S-parameters of the verification devices. The simulations were performed using its frequency-domain solver with a tetrahedral mesh and adaptive mesh refinement to ensure 2% ΔS convergence. The waveguide surfaces were modeled as gold, using the default conductivity value of $\sigma = 4.56 \times 10^7$S/m from the software's material library, to correspond with the gold-plated surfaces of the physical waveguide sections.

A CCW can be easily realized using any short section of waveguide line for the same frequency band (WM-570 in this case) with 90° rotation. As the conventional IEEE 1758-2a waveguide flange is axis-symmetric, the CCW does not require any additional adapters or modifications [9], [10]. Here, a 655 μm calibration line standard was selected.

The RAW can also be easily implemented by using any short section of waveguide line with a smaller aperture size (i.e., a waveguide line section at a higher frequency band).

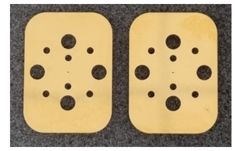

Fig. 2. WM-380 waveguide sections: short line (left) and long line (right).

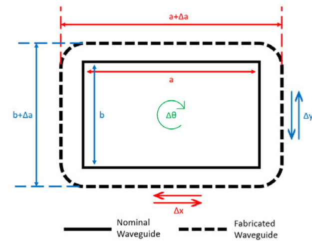

Fig. 3. Illustrated in-plane imperfections and misalignments of a rectangular waveguide flange aperture.

In this study, two WM-380 lines with nominal lengths of 432 μm multiplly symbol 568 μm were employed, as shown in Fig. 2. These lines were also manufactured by Swiss-to-12, to be used as calibration standards for the WM-380 frequency band (500–750 GHz). The lines have nominal aperture dimensions of 380 μm × 190 μm and are expected to show partial out-of-band characteristics at low frequencies (between 330 and ~390 GHz) and in-band characteristics at high frequencies (between ~390 and 500 GHz). This setup allows a single device to verify the VNA's performance in two distinct dynamic regimes.

Due to fabrication tolerances, manufactured waveguide sections are expected to have several imperfections associated with dimensions of the waveguide and the flange structure [11], as illustrated in Fig. 3. Here, seven different imperfections are considered, associated with the waveguide's physical dimensions. Deviations in the broad wall, narrow wall, and length dimensions are $\Delta a, \Delta b$, and Δl, respectively. Imperfections due to horizontal, vertical, and rotational misalignments are $\Delta x, \Delta y$, and $\Delta\theta$, respectively. Finally, the corner rounding radius R is also considered. Previously, a dimensional analysis of WM-380 waveguide sections [11], provided by Swiss-to-12, showed that the samples have much better dimensional tolerance than the standard Grade 1.0 waveguide specifications [9]. Therefore, in this study, the maximum tolerance (T_i) due to these imperfections and misalignment values (Grade 1.0) from [9] and [10] is adopted.

As the tolerance values for each imperfection are considered worst case and are characterized by a uniform probability distribution, the local standard uncertainties $u(T_i)$ can be established as follows [12]:

$$u(T_i) = \frac{T_i}{\sqrt{3}}. \tag{1}$$

The tolerances adopted for this work and the corresponding local standard uncertainties of the CCW and RAW are shown in Tables I and II, respectively.

The deviation in the magnitude of the transmission and reflection coefficients, due to the local uncertainties of the

TABLE I

DIMENSIONAL IMPERFECTIONS AND MISALIGNMENT VALUES OF WM-570 CCW

Imperfection i		Tolerance T_i	Local Standard Uncertainty $u(T_i)$
1	Δa	± 0.0057 mm	± 0.0033 mm
2	Δb	± 0.0057 mm	± 0.0033 mm
3	Δl	± 0.01 mm	± 0.0058 mm
4	Δx	± 0.0025 mm	± 0.0014 mm
5	Δy	± 0.0025 mm	± 0.0014 mm
6	$\Delta\theta$	± 0.40°	± 0.23°
7	R	0.020 mm	0.012 mm

TABLE II

DIMENSIONAL IMPERFECTIONS AND MISALIGNMENT VALUES OF WM-380 RAW

Imperfection i		Tolerance T_i	Local Standard Uncertainty $u(T_i)$
1	Δa	± 0.0038 mm	± 0.0022mm
2	Δb	± 0.0038 mm	± 0.0022 mm
3	Δl	± 0.01 mm	± 0.0058 mm
4	Δx	± 0.0025 mm	± 0.0014 mm
5	Δy	± 0.0020 mm	± 0.0012 mm
6	$\Delta\theta$	± 0.40°	± 0.23°
7	R	0.020 mm	0.012 mm

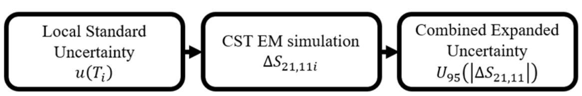

Fig. 4. Simulated uncertainty contributions due to local standard uncertainty factors.

CCW and RAWs, was predicted from EM simulations. Nominal WM-380 and WM-570 waveguide dimensions and the local standard uncertainties from Tables I and II are used in the simulation. The results were then combined to calculate the expanded uncertainty with 95% coverage, U_{95}, as follows:

$$U_{95}\left(\left|\Delta S_{21,11}\right|\right) = k \cdot \sqrt{\sum_{i=1}^{7} \left|\Delta S_{21,11i}\right|^2} \quad (2)$$

where $k = 2$ is the coverage factor. A summary of the workflow for extracting the expanded uncertainty is depicted in Fig. 4.

III. SIMULATION AND MEASUREMENT RESULTS

In this section, measured results are compared with the simulated predictions. A Rohde & Schwarz (R&S) ZVA 67 VNA with a pair of ZVA-Z500 frequency extension modules, one for each port, is used for the S-parameter measurements. As mentioned in Section II, a 1/4-wave TRL calibration scheme was performed using the Swiss-to-12 WM-570 calibration kit. The detailed measurement setup can be found in [13].

The comparison presented in this section distinguishes between the verification device's geometric tolerances and the measurement instrument's residual errors. The expanded uncertainty bands calculated in Section II solely represent the geometric limits of the waveguide standards. While a complete uncertainty budget typically includes VNA residual errors (e.g., system noise floor, linearity, and drift), this work adopts a *fit-for-purpose* approach that is suitable for non-NMI routine laboratory verification. Therefore, the verification criterion is primarily defined by these mechanical manufacturing tolerances. However, to account for instrument-level factors such as VNA trace stability, a conservative buffer (<0.5 dB [14]) is added to the simulated tolerance envelope. Agreement between the raw measurement data and this combined envelope serves as the verification criterion.

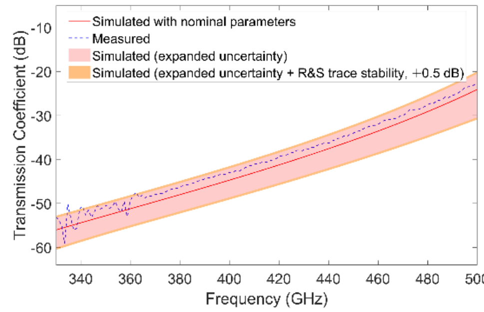

Fig. 5. Measured and simulated transmission coefficient of the CCW.

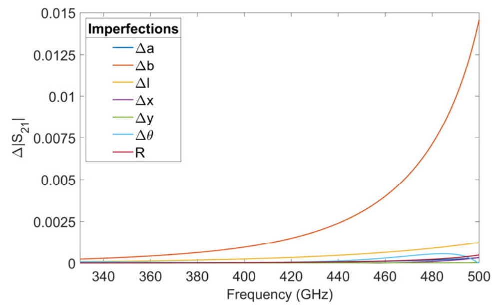

Fig. 6. Simulated uncertainty contributions to transmission coefficients due to local standard uncertainty factors.

A. Cross-Connected Waveguide

Measured and simulated transmission coefficients for the CCW, over the frequency range of 330–500 GHz, are shown in Fig. 5. The predicted expanded uncertainty and the VNA trace stability intervals are also shown in Fig. 5. The measured and simulated results are in good agreement across this frequency range. Also, the measured transmission coefficient lies within the expanded uncertainty interval, calculated from simulated results. Note that the oscillatory behavior in the 330–365 GHz range is attributed to VNA frequency extender characteristics near the band edge. The measurements still remain well within the calculated uncertainty envelope, validating this method. Also, a small systematic deviation is observed between the measured and simulated results. This trend is likely due to the assumption of the idealized geometry of the CCW in the nominal simulation. In practice, manufacturing tolerances may introduce slight geometric asymmetries, resulting in the higher transmission levels observed in the measurement.

Fig. 6 shows simulated uncertainties in the transmission coefficient due to the imperfections quoted in Table I. It can be seen that the narrow wall imperfection Δb of the CCW is the most significant contribution to uncertainty. This is physically

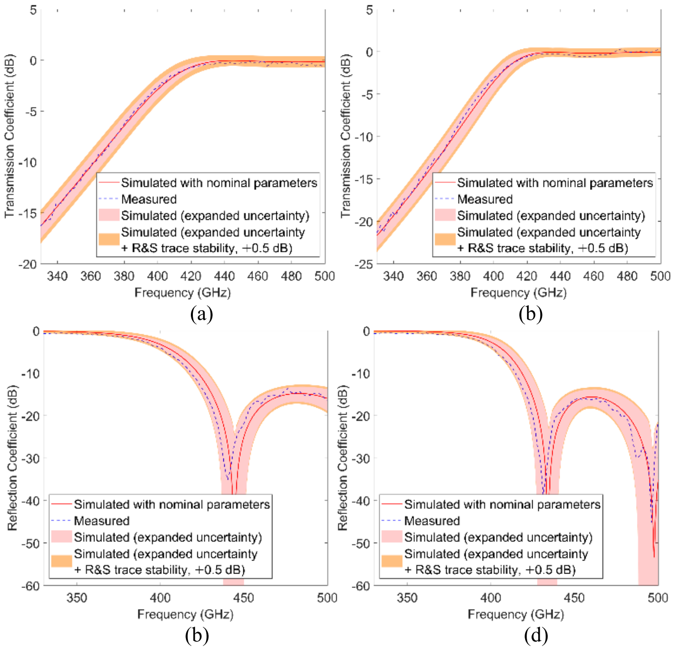

Fig. 7. RAW. (a) Short line (transmission), (b) long line (transmission), (c) short line (reflection), and (d) long line (reflection).

expected for the cross-connected configuration. Since the waveguide is rotated by 90°, the broad wall dimension a of one port aligns with the narrow wall of the other. A deviation in the narrow wall height directly alters the wave impedance and the step height of the discontinuity at the interface. Furthermore, since the b dimension is significantly smaller than a, a fixed manufacturing tolerance represents a larger percentage error, resulting in a more severe impact on transmission.

B. Reduced Aperture Waveguide

Measured and simulated transmission and reflection coefficients of the short and long RAWs are shown in Fig. 7. The predicted expanded uncertainty interval is also shown. The RAW acts as a high-pass filter, governed by the cutoff frequency of this central WM-380 section (~390 GHz). Inside the stopband for the RAW (i.e., 330 to ~390 GHz), measured and simulated transmission coefficient results show excellent agreement in Fig. 7(a) and (b). In this frequency range, the measured transmission coefficient lies within the expanded uncertainty interval, calculated from simulated results. However, inside the passband for the RAW (i.e., ~390 to 500 GHz), the deviation between measured and simulated transmission coefficient slightly increases.

For the reflection coefficients, the simulated expanded uncertainty provides a very good coverage interval within the in-band frequency range, as shown in Fig. 7(c) and (d). This is expected as imperfections associated with the dimensions of the waveguide are not the dominating factors for the uncertainty when the magnitudes of the transmission and reflection coefficients are close to 0 dB (i.e., high transmission or reflection). In these regions, factors such as VNA trace stability become more significant (e.g., <0.5 dB for the ZVA-Z500 [14]).

IV. Conclusion

In this article, a simulation-based methodology for verifying (sub-)terahertz S-parameter measurements has been demonstrated using simple, calculable waveguide devices. A key finding is that even without access to verification standards that have undergone rigorous and costly dimensional analysis, full-wave EM simulation that accounts for nominal manufacturing tolerances can provide a reliable uncertainty envelope for measurement verification. The measured responses for both the cross-connected and reduced-aperture waveguides show excellent agreement with the simulated predictions, falling well within the calculated uncertainty. This work confirms that leveraging EM simulation with simple waveguide components is a cost-effective and practical approach to validating VNA calibrations at (sub-)THz frequencies for routine laboratory measurements where rigorous primary-level accuracy is not required.

Acknowledgment

The authors would like to thank the late Prof. N. Klein for his support and Dr. S. Ramadan for arranging the measurement, both at Imperial College London.

References

[1] A. Rumiantsev and N. Ridler, “VNA calibration,” *IEEE Microw. Mag.*, vol. 9, no. 3, pp. 86–99, Jun. 2008.

[2] N. M. Ridler and M. J. Salter, “Cross-connected waveguide lines as standards for millimeter- and submillimeter-wave vector network analyzers,” in *Proc. 81st ARFTG Microw. Meas. Conf.*, Seattle, WA, USA, Jun. 2013, pp. 1–7.

[3] M. J. Salter and N. M. Ridler, “Use of reduced aperture waveguide as a calculable standard for the verification of millimetre-wave vector network analyzers,” in *Proc. 44th Eur. Microw. Conf.*, Rome, Italy, Oct. 2014, pp. 750–753.

[4] H.-J. Eul and B. Schiek, “A generalized theory and new calibration procedures for network analyzer self-calibration,” *IEEE Trans. Microw. Theory Techn.*, vol. 39, no. 4, pp. 724–731, Apr. 1991.

[5] G. F. Engen and C. A. Hoer, “Thru-reflect-line: An improved technique for calibrating the dual six-port automatic network analyzer,” *IEEE Trans. Microw. Theory Techn.*, vol. MTT-27, no. 12, pp. 987–993, Dec. 1979.

[6] C. A. Hoer, “Choosing line lengths for calibrating network analyzers,” *IEEE Trans. Microw. Theory Techn.*, vol. MTT-31, no. 1, pp. 76–78, Jan. 1983.

[7] N. M. Ridler, “Choosing line lengths for calibrating waveguide vector network analysers at millimetre and sub-millimetre wavelengths,” NPL, Nat. Phys. Lab., Teddington, U.K., Tech. Rep. TQE 5, Mar. 2009.

[8] N. M. Ridler, R. G. Clarke, C. Li, and M. J. Salter, “Strategies for traceable submillimeter-wave vector network analyzer,” *IEEE Trans. THz Sci. Technol.*, vol. 9, no. 4, pp. 392–398, Jul. 2019.

[9] *IEEE Standard for Rectangular Metallic Waveguides and Their Interface for Frequencies of 110 GHz and Above—Part 1: Frequency Bands and Waveguide Dimensions*, Standard 1785.1-2012, 2012.

[10] *IEEE Standard for Rectangular Metallic Waveguides and Their Interfaces for Frequencies of 110 GHz and Above—Part 2: Waveguide Interfaces*, Standard IEEE 1785.2-2016, 2016.

[11] N. M. Ridler, S. Johny, M. J. Salter, X. Shang, W. Sun, and A. Wilson, “Establishing waveguide lines as primary standards for scattering parameter measurements at submillimetre wavelengths,” *Metrologia*, vol. 58, no. 1, pp. 1–13, Jan. 2021.

[12] *The Expression of Uncertainty, and Confidence in Measurement, M 3003, Ed. 4*, United Kingdom Accreditation Service (UKAS), Staines-upon-Thames, U.K., Nov. 2019.

[13] L. Zhu et al., “3-D printed THz waveguide components,” *IEEE Access*, vol. 11, pp. 79073–79086, 2023.

[14] S. Rohde, *R&SZVA-Zxx Millimeter-Wave Converters Specifications*, document 5124-2033-22, Version 22.00, May 2021. [Online]. Available: https://scdn.rohde-schwarz.com/ur/pws/dl_downloads/dl_common_library/dl_brochures_and_datasheets/pdf_1/ZVA-Zxx_dat-sw_en_5214-2033-22_v2200.pdf

Sang-Hee Shin (Member, IEEE) received the M.Eng. degree in aeronautical engineering and the Ph.D. degree in electrical and electronic engineering from Imperial College London, London, U.K., in 2018 and 2022, respectively.

He was a Higher Research Scientist at the Department of Electromagnetic and Electrochemical Technologies, National Physical Laboratory (NPL), Teddington, U.K. He is currently an Assistant Professor with the Department of Quantum Information Engineering, Sungkyunkwan University (SKKU), Suwon, South Korea. His research interests focus on the intersection of high-frequency metrology and quantum technology, specifically the design and manufacturing of RF and microwave devices for cryogenic quantum computing applications.

Stepan Lucyszyn (Fellow, IEEE) received the Ph.D. degree in electronic engineering from King's College London, University of London, London, U.K., in 1992, and the D.Sc. degree (Higher Doctorate) in millimeter-wave and terahertz electronics from Imperial College London, London, in 2010.

He is currently a Professor of millimeter-wave systems with Imperial College London. He has co-authored well over 200 articles and 12 book chapters in applied physics and electronic engineering. He was appointed as an IEEE Distinguished Microwave Lecturer from 2010 to 2013 and co-founded Imperial College London spin-out company Drayson Wireless Ltd., London, in 2014.

Dr. Lucyszyn was a fellow of the Institution of Electrical Engineers and also the Institute of Physics, U.K., in 2005. He became a fellow of the Electromagnetics Academy and the Institute of Electrical and Electronics Engineers, USA, in 2008 and 2014, respectively. He was elected as a fellow of the Royal Academy of Engineering, U.K., in 2023. In 2022, he and his team at Imperial College London won Junkosha's Inaugural Technology Innovator of the Year Award for the Microwave and Millimeter Wave category for their work on 3-D printing.

Nick M. Ridler (Fellow, IEEE) received the B.Sc. degree from King's College London, London, U.K., in 1981.

He is currently the Head of Science for electromagnetic and electrochemical technologies at the National Physical Laboratory (NPL), Teddington, U.K. He is also an Honorary Professor at the University of Glasgow, Glasgow, U.K., and the University of Liverpool, Liverpool, U.K., and a Visiting Professor at the University of Kent, Canterbury, U.K., the University of Leeds, Leeds, U.K., and the University of Strathclyde, Glasgow, U.K. He is a Director of the European Microwave Association (EuMA) and a Non-Executive Director of LA Techniques Ltd., Surbiton, U.K. He has more than 40 years of experience working in industrial, government, and academic research establishments. His research interests include developing accurate electromagnetic measurement techniques at high frequencies (i.e., from approximately 1 kHz to 1 THz).

Prof. Ridler is an NPL Fellow and a fellow of the U.K. Royal Academy of Engineering (FREng), the Institution of Engineering and Technology (FIET), and the Institute of Physics (FInstP). He was the General Chair of the 2021 European Microwave Week.